arXiv:hep-th/0605175v2 5 Aug 2007

Global Currents, Phase Transitions and Chiral Symmetry Breaking in Large N_c Gauge Theory

Tameem Albash, Veselin Filev, Clifford V. Johnson[1], Arnab Kundu

Department of Physics and Astronomy
University of Southern California
Los Angeles, CA 90089-0484, U.S.A.

`albash, filev, johnson1, akundu @usc.edu`

Abstract

We study, using a gravity dual, the finite temperature dynamics of $SU(N_c)$ gauge theory for large N_c, with fundamental quark flavours in a quenched approximation, in the presence of a fixed charge under a global current. We observe several notable phenomena. There is a first order phase transition where the quark condensate jumps discontinuously at finite quark mass, generalizing similar transitions seen at zero charge. We find a non–zero condensate at zero quark mass above a critical value of the charge, corresponding to an analogue of spontaneous chiral symmetry breaking at finite number density. We find that the spectrum of mesons contains the expected associated Goldstone ("pion") degrees of freedom with a mass dependence on the quark mass that is consistent with the Gell-Mann–Oakes–Renner relation. Our tool in these studies is holography, the string dual of the gauge theory being the geometry of N_c spinning D3–branes at finite temperature, probed by a D7–brane.

---

[1] Also, Visiting Professor at the Centre for Particle Theory, Department of Mathematical Sciences, University of Durham, Durham DH1 3LE, England, U.K.

1 Introduction and Conclusions

There is great interest in understanding the phase structure of Quantum Chromodynamics (QCD). There are various regions of the (μ_B, T) phase diagram (T is temperature and μ_B is a chemical potential for baryon number) which are extremely hard to model theoretically using traditional field theory techniques. Some of these regimes are being probed experimentally, and so there is additional interest in obtaining better theoretical understanding from an immediate phenomenological point of view.

For almost a decade, progress in understanding the dynamics of extended objects in string theory has enabled several new techniques–and a fresh and powerful new perspective–to be brought to the study of strongly coupled gauge theory. The techniques were sharpened further (for large number of colours, N_c,) with holographic examples such as the AdS/CFT correspondence, and the study of gauge/gravity duals (or, more properly, gauge/string duals) has proven to be a fruitful and often elegant pursuit.

Not long after the birth of AdS/CFT[1, 2, 3], where the finite temperature phase structure of $\mathcal{N} = 4$ $SU(N_c)$ (at large N_c) was understood in terms of the thermodynamics of Schwarzschild black holes in AdS[2, 4], it was recognized[5] that progress could be made in understading the properties of gauge theories in the presence of a global current, akin to a chemical potential for baryon number or isospin, by studying the physics of charged black holes, such as Riessner–Nordstrom[5, 6], or more general charged black holes with non–trivial scalars[7], in AdS.

The resulting (μ, T) or (q, T) phase diagrams (where q is conjugate to μ–the analogue of Baryon number) of the $\mathcal{N} = 4$ guage theory were found to be rather rich, with *e.g.,* a first order phase transition line, and even a second order critical point in the (q, T) plane[5, 6]. This led to the hope[1] that such studies might lead to insights into the physics of the QCD phase diagram. The idea is that studies of the effect of the global $U(1)$ symmetry–even though it is not exactly baryon number–might lead to physics in the same universality class as the more realistic gauge theories, giving insight into QCD at finite temperature and density.

A more firm footing for this idea should be obtained by the study of those dynamics in the presence of fundamental flavours of quark, a key feature of QCD that distinguishes it from the $\mathcal{N} = 4$ gauge theory (which of course only has adjoint matter of very specific types and quantities allowed by supersymmetry). While it is notoriously difficult to study this problem as a string dual —so far— it is known[8] how to place fundamental flavours into the theory, in the limit $N_c \gg N_f$. This is a sort of "quenched" limit where the quarks feel the gauge dynamics but whose presence does not effect the physics (*i.e.,* the quarks do not back–react).

---

[1] C. V. Johnson, various seminars, 2000

While this limit cannot capture a great deal of detailed QCD physics, it is hoped that it may well provide valuable clues in the study of the phase structure and will certainly be an instructive step along the path to fully understanding the case of fully interacting dynamical quarks.

The global symmetries in question in the case of the $\mathcal{N}=4$ theory live in the $U(1)^3$ subgroup of the large $SO(6) \subset SU(4)$ R–symmetry enjoyed by the theory. In the string dual this corresponds to that fact that the D3–branes (on whose worldvolume the gauge theory resides) have an $\mathbb{R}^6$ transverse to them, In the decoupling limit that gives the AdS/CFT duality, they correspond to a subset of the $SO(6)$ isometries of the explicit S^5 of the $\text{AdS}_5 \times S^5$ spacetime where the dual string theory propagates.

Fundamental dynamical quarks enter the story as D7–brane probes of the geometry. The $\mathcal{N}=4$ supersymmetry is now replaced by $\mathcal{N}=2$ and the quarks lie in hypermultiplets. The $\mathbb{R}^6$ now breaks into an $\mathbb{R}^2$ transverse to both the D3–branes and the D7–branes, and an $\mathbb{R}^4$ transverse to the D3–branes, but internal to the D7–branes.

In the probe limit in question, the quarks are the ends of the strings stretching from the D7–branes to the D3–branes, their masses being set by the distance between the two sets of branes in the $\mathbb{R}^2$. In the decoupling limit (where the N_c D–branes have been replaced by $\text{AdS}_5 \times S^5$ geometry), the location in the plane transverse to the D7–brane controls the quark mass and a condensate of quarks, according to[9]:

$$\lim_{u\to\infty} L(u) \sim m + \frac{c}{u^2} + \cdots \ , \tag{1}$$

where $m = 2\pi\alpha' m_q$ (the bare quark mass) and $-c = \langle\bar{\psi}\psi\rangle/(8\pi^3\alpha' N_f \tau_{\text{D7}})$ (the quark condensate), u is a radial coordinate in the decoupling limit, and $N_f = 1$ in this paper.

The condensate actually breaks the $U(1)$ symmetry corresponding to rotations in the $\mathbb{R}^2$, that acts chirally on the ψ fields. We explored the allowed values of the condensate $-c$ as a function of quark mass m at finite temperature T (where supersymmetry is broken), and with the system charged an amount q under a global $U(1)$ current. We did two cases. The first is the chiral current associated with rotations transverse to the D7–branes, and the second is a $U(1)$ that mixes transverse and parallel rotations.

We found a rich structure, upon which we will report in this paper. We found that there are generalizations of the first order phase transition already observed (and extensively studied, see refs.[10, 11, 12, 13, 14, 15]) at $q = 0$ for this case. In addition, we found that at finite q a new phase appears where there is a non–zero condensate at zero quark mass m. This is an example of spontaneous chiral symmetry breaking in the presence of an analogue of finite fixed baryon number or isospin charge.

We study the meson spectrum of our model and identify the massless "pions" (it is really a slight misnomer — see ref.[9]) which play the role of the Goldstone bosons of the chiral symmetry breaking. We study the behaviour of the pion mass as a function of quark mass m and find that it obeys the Gell-Mann–Oakes–Renner relation[16]. Crucially, we also verify that away from the range of q where the symmetry breaking is present, the meson has no massless particle at $m = 0$, confirming our identification.

2 Spinning D3-branes

To source subgroups of the $U(1)^3 \subset SO(6)$ global symmetries corresponding to rotations in the transverse $\mathbb{R}^6$, we consider D3–branes with angular momentum. The supergravity description/metric for spinning D3–branes is[17, 18]:

$$\begin{aligned} ds^2 &= H_3^{-1/2}\left\{-\left(1-\frac{r_H^4}{r^4\Delta}\right)dt^2 + d\vec{x}\cdot d\vec{x}\right\} + H_3^{1/2}\left\{\frac{\Delta dr^2}{\mathcal{H}_1\mathcal{H}_2\mathcal{H}_3 - \frac{r_H^4}{r^4}} + r^2\sum_{i=1}^{3}\mathcal{H}_i\left(d\mu_i^2 + \mu_i^2 d\phi_i^2\right)\right. \\ &\quad \left. -\frac{2r_H^4\cosh(\beta_4)}{r^4 H_3\Delta}dt\left(\sum_{i=1}^{3}R_i\mu_i^2 d\phi_i\right) + \frac{r_H^4}{r^4}\frac{1}{H_3\Delta}\left(\sum_{i=1}^{3}R_i\mu_i^2 d\phi_i\right)^2\right\} , \end{aligned} \tag{2}$$

where:

$$\begin{aligned} \Delta &= \mathcal{H}_1\mathcal{H}_2\mathcal{H}_3\sum_{i=1}^{3}\frac{\mu_i^2}{\mathcal{H}_i} \\ H_3 &= 1 + \frac{r_H^4}{r^4}\frac{\sinh(\beta_3)}{\Delta} = 1 + \frac{\alpha_3 r_3^4}{\Delta r^4} \\ \mathcal{H}_i &= 1 + \frac{\ell_i^2}{r^2} \\ r_3^4 &= 4\pi g_s N\alpha'^2 = \alpha'^2\hat{r}^4 \\ \alpha_3 &= \sqrt{1+\left(\frac{r_H}{2r_3}\right)^8} - \left(\frac{r_H}{2r_3}\right)^4 . \end{aligned}$$

In order to explore the decoupling limit ($\alpha' \to 0$), which we are interested in, we define:

$$r = \alpha' u , \quad r_H = \alpha' u_H, \quad \ell_i = \alpha' q_i ,$$

such that:

$$\begin{aligned}\frac{\alpha_3 r_3^4}{r_H^4} &\to \frac{\hat{r}_3^4}{\alpha'^2 u_H^2}\ , \quad \sinh(\beta_3) \to \frac{\hat{r}_3^2}{\alpha' u_H^2}\ , \\ \mathcal{H}_i &\to 1+\frac{q_i^2}{u^2}\ , \quad H_3 \to \frac{\hat{r}_3^4}{\alpha'^2 u^4 \Delta}\ .\end{aligned}$$

With these definitions, in the decoupling limit, the metric is:

$$\begin{aligned}ds^2/\alpha' &= \Delta^{\frac{1}{2}}\left\{-\left(\mathcal{H}_1\mathcal{H}_2\mathcal{H}_3\right)^{-1} f dt^2 + f^{-1}du^2 + \frac{u^2}{R^2}d\vec{x}\cdot d\vec{x}\right\} \\ &\quad +\Delta^{-\frac{1}{2}}\left\{\sum_{i=1}^{3}\mathcal{H}_i\mu_i^2\left(Rd\phi_i - Adt\right)^2 + R^2\mathcal{H}_i d\mu_i^2\right\}\ , \end{aligned} \tag{3}$$

where we have defined:

$$R = \hat{r}_3\ , \quad f = \frac{u^2}{R^2}\mathcal{H}_1\mathcal{H}_2\mathcal{H}_3 - \frac{u_H^4}{u^2R^2}\ , \quad \text{and} \quad A = \frac{u_H^2}{R\mathcal{H}_i}\frac{q_i}{u^2}\ . \tag{4}$$

There are two different cases that we consider:

1. A single charge in the ϕ_1 direction: $q_1 = q$ and $q_2 = q_3 = 0$. This case is a useful test case since it is the simplest problem to explore and provides valuable insight into the next, more complicated case.

2. Three equal charges: $q_1 = q_2 = q_3 = q$. This case is of greater interest since the supergravity metric, upon compactification, corresponds to the AdS–Reissner–Nordstrom black hole[5] (the previous case gives charged black holes with an extra scalar field excited[7]).

3 Single Charge

For the single charge case, we choose $q_1 = q$ and $q_2 = q_3 = 0$ in equation (3), and the metric becomes:

$$\begin{aligned}ds^2/\alpha' &= \Delta^{1/2}\left\{-\mathcal{H}^{-1} f dt^2 + \frac{u^2}{R^2}d\vec{x}\cdot d\vec{x}\right\} + \Delta^{1/2}\left\{f^{-1}du^2 + R^2 d\theta^2\right\} \\ &\quad +\Delta^{-1/2}\left\{\mathcal{H}\sin^2\theta\left(Rd\phi_1 - Adt\right)^2 + R^2\cos^2\theta d\Omega_3^2\right\}\ , \end{aligned} \tag{5}$$

where

$$f = \frac{u^2}{R^2}\mathcal{H} - \frac{u_H^4}{u^2R^2}\ , \quad \mathcal{H} = 1+\frac{q^2}{u^2}\ , \quad A = \frac{u_H^2 q}{Ru^2\mathcal{H}}\ , \quad \Delta = \sin^2\theta + \mathcal{H}\cos^2\theta\ . \tag{6}$$

Although there is a change of variables that allows us to rewrite this metric in a more conventional form, it will be computationally convenient to work with the metric in equation (5). In order to introduce dynamical quarks into our gauge theory, we probe the geometry with D7–branes [8]. We choose the coordinates (θ, ϕ_1) to be the transverse coordinates to the D7–brane. However, we will define radial coordinates in the R^6–subspace transverse to the D–3 branes via:

$$\rho = u\cos\theta \ , \quad L = u\sin\theta \ . \tag{7}$$

Although these radial coordinates are not transverse to each other, the non-zero $G_{L\rho}$ component of the metric vanishes at the asymptotic boundary. Therefore, by expanding:

$$L = m + \frac{c}{u^2} + O\left(\frac{1}{u^4}\right) \ , \tag{8}$$

we can still make sense of the coefficient m as being the asymptotic separation of the D–3 and D–7 branes. This will allow us to extract the bare quark mass and the condensate value. It should be noted however that, unlike the zero charge case considered in refs.[11, 13], we cannot directly identify the coefficient c with the quark condensate. The correct identification can be made after an appropriate change of variables that restores the S^5 symmetry of the geometry at the asymptotic boundary. We will explicitly show this later.

We choose an ansatz $\theta = \theta(u)$ and $\partial_\mu\phi_1 = 0$. With these choices, the worldvolume of the D7–brane is given by:

$$\sqrt{-\det g} = (\det S_3)^{1/2}\, u^2\cos^3\theta \left|\frac{1}{f\mathcal{H}}\left(fq^2\cos^2\theta + \left(f - A^2\mathcal{H}^2\sin^2\theta\right)u^2\right)\left(1 + fR^2(\theta')^2\right)\right|^{1/2} \ . \tag{9}$$

From here, we see that the worldvolume goes to zero for two particular cases:

1. $\theta = \pi/2$. This case is akin to the Karch-Katz like solutions described in ref.[11].
2. $\left|fq^2\cos^2\theta + \left(f - A^2\mathcal{H}^2\sin^2\theta\right)u^2\right| = 0$. This is akin to the condensate solutions described in ref.[11]. Note the absolute value sign in (9). This means that although the world–volume goes to zero at this point, the D7–brane does not actually end there. The vanishing is a result of the coordinates we are using; the D7–brane continues through and terminates on the event horizon defined by $G^{uu} = 0$. We are only interested in D7–brane embeddings that are smooth (no kinks) across this locus, as they correspond to the lowest energy solutions. This condition of smoothness, which has only been checked numerically, is only satisfied for a particular boundary condition for our scalar fields on this locus, which we describe below.

We solve the equation of motion for θ numerically using a shooting technique. We use $R = 1$ and $u_H = 1$ throughout our numerical calculations. Such a choice corresponds to measuring distances in units of the AdS radius and to fixing the mass of the black hole, respecively. It has become customary in the field [10, 12, 15] to shoot from the event horizon towards infinity. Using IR boundary conditions for the uncharged case has meant that the correct UV boundary values are achieved automatically, and the bare quark mass and condensate are extracted in this way. For the charged case, because the ergosphere and the event horizon do not coincide, this introduces a new complication. For $\theta < \pi/2$, near the event horizon, the equation of motion for the embedding resembles:

$$\sqrt{f}\left(A_1\theta''(z) + A_2\theta'(z)^2\right) + \frac{1}{\sqrt{f}}\left(A_3\theta'(z) + A_4\right) \;=\; 0 \tag{10}$$

where A_i are functions of $z = u^{-2}$ and $\theta(z)$. Since $f \to 0$ at the event horizon, we use equation (10) to obtain the necessary boundary condition, which is depicted in figure 1. However,

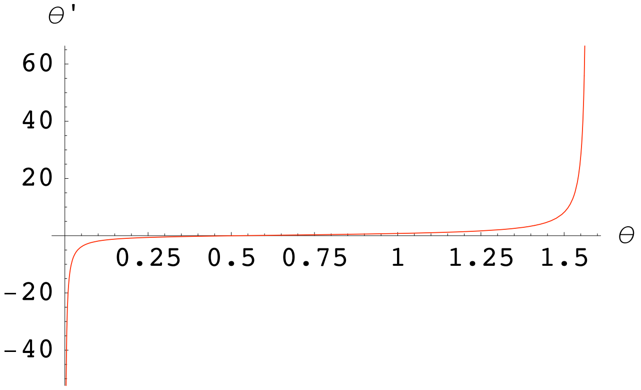

Figure 1: Boundary condition at the event horizon for $q = 0.5$.

if we use this boundary condition to shoot to infinity, we find that $\theta'(z)$ diverges at the locus of points where the worldvolume vanishes. At first glance, this may not be a problem, since it is a necessary condition if we wish to have a regular, non–zero worldvolume across the locus. However, in this case, the worldvolume diverges at the pseudo-horizon. This results in the D7–brane embedding to curve back on itself, as shown in figure 2. We argue that these solutions do not correspond to physical D7–brane embeddings, and, therefore, the boundary conditions specified at the event horizon are not the ones we are interested in. We get similar results if we try to force the worldvolume to be regular and non–zero across the same locus of points. Therefore, we impose a new "physical" condition on our embeddings; we want $\theta'(z)$ to be at least continuously differentiable across the locus of vanishing worldvolume. In order to

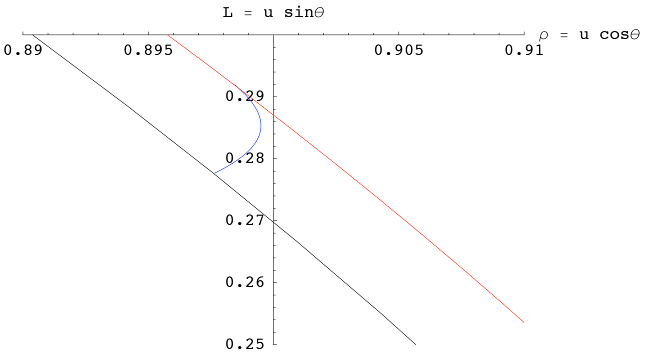

Figure 2: Shooting from the event horizon ($q = 0.5$) results in embeddings curving back . The left–most (black) line is the event horizon; the right–most (red) line is the vanishing worlvolume locus. The (blue) curve in between is the embedding solution.

figure out the appropriate boundary conditions at this locus of points, we study the equation of motion near the locus:

$$\sqrt{F}\left(B_1\theta''(z)+B_2\theta'(z)+B_3\theta'(z)^2+B_4\theta'(z)^3\right)+\frac{C_1}{\sqrt{F}}\left(B_5\theta'(z)+B_6\right) \;=\; -0\ , \qquad (11)$$

where B_i depends on z and $\theta(z)$, and C_1 is a strictly positive function of $z, \theta'(z)^2$. Since $F \to 0$ at the locus of vanishing worldvolume, we use this equation to obtain the necessary boundary condition, which is depicted in figure 3. Therefore, for $\theta < \pi/2$, we shoot from the

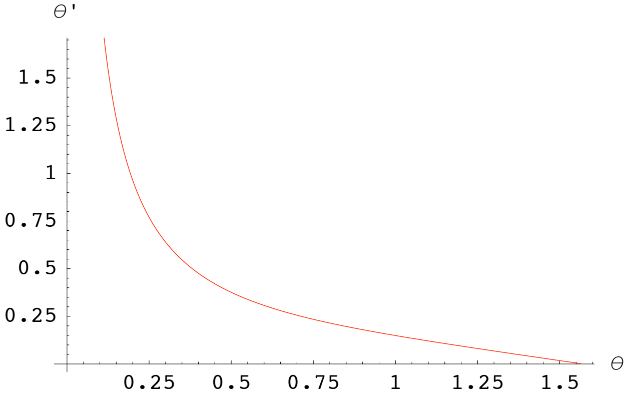

Figure 3: Boundary condition at the pseudo-horizon for $q = 0.5$.

locus described in point 2 above–which is not where the D7–brane ends, in knowledge that we are able to "sew" the rest of the D7–brane that ends on the event horizon. Two examples of this sewing process are shown in figure 4 to illustrate that it can be done, and we refrain from plotting the sewed solutions on future plots. We use the boundary conditions depicted in figure 3. For $\theta = \pi/2$, this corresponds to shooting from the location described in point 1

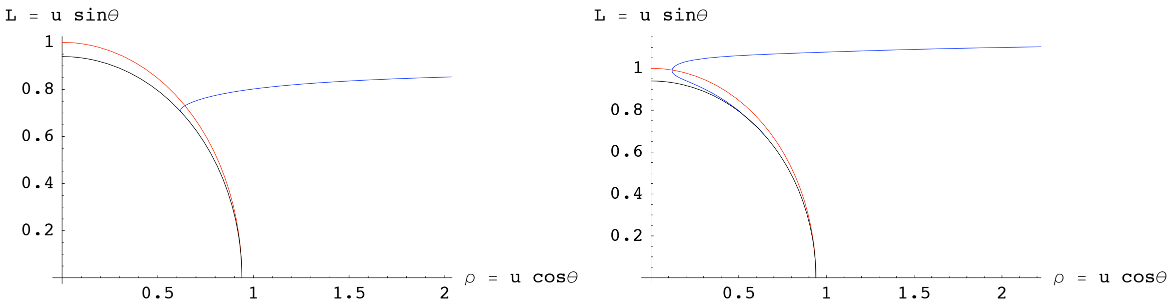

(a)

(b)

Figure 4: Sewing of solutions for one single charge ($q = 0.5$) in the transverse direction. The black (inner most) curve corresponds to the event horizon, the red (slightly above) curve to the shooting locus, and the blue (extends to the right) curve to the D7–brane embedding.

above, where the D7–brane has ended. The boundary condition is given by:

$$\begin{aligned} \theta &= \pi/2 \\ \theta'\big|_{\theta=\pi/2} &= \infty\ . \end{aligned} \qquad (12)$$

These boundary conditions were also used in reference [12]; it is a result of requiring the absence of conifold singularities as the S^3 that the D7–brane wraps shrinks to zero size.
Figure 5(a) shows examples of the condensate and Karch–Katz-like solutions as they approach their respective end points. It is important to notice that in figure 5(b), the Karch–Katz-like solutions have a slope of $q^2/2$ for large m, so this choice of the constant c is not proportional to the condensate, as we remarked earlier. This is a result of our choice of coordinates in the expansion of L as given in equation (8), for which:

$$\langle\bar{\psi}\psi\rangle \sim -c - \frac{q^2}{2}m\ . \qquad (13)$$

In order to see this, we recall that for the zero charge case (*i.e.,* the AdS Schwarzschild black hole studied in ref.[11]), as $u \to \infty$, we have $L \sim (m + \frac{c}{u^2})$; the constant c is proportional to the quark condensate as shown by ref.[9]. The key geometric difference between the charged and uncharged case is that the S^5 gets distorted due to the presence of the charge q. In order to be able to identify the condensate, we want to restore the symmetry of the S^5 as much as possible as we move away from the horizon.

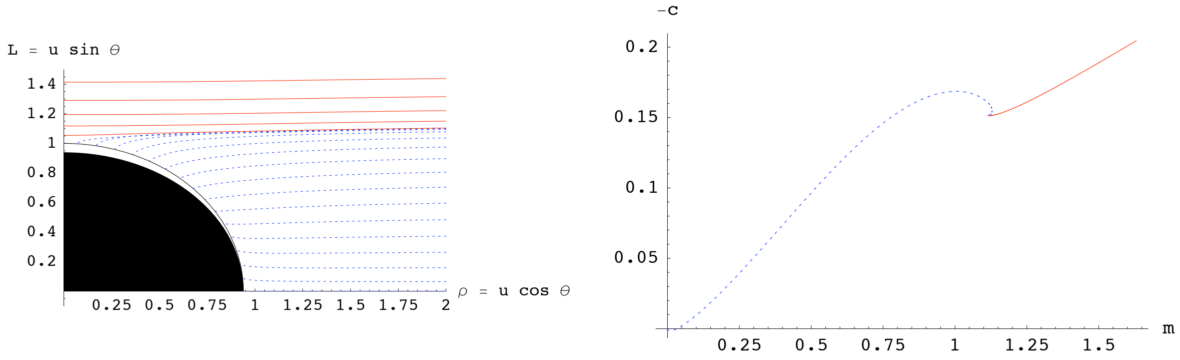

(a) (b)

Figure 5: Solutions for one single charge ($q = 0.5$) in the transverse direction

By looking at the distorted S^5 part in equation (3), one can see that, as we start moving away from the horizon (i.e. when we see the effect of u_H less and less), it starts conformally looking like:

$$ds_{S_5}{}^2 = \sum_{i=1}^{3} \mathcal{H}_i \left(d\mu_i^2 + d\phi_i^2 \mu_i^2 \right) , \tag{14}$$

where

$$\mu_1 = \sin\theta , \quad \mu_2 = \cos\theta \sin\psi , \quad \mu_3 = \cos\theta \cos\psi . \tag{15}$$

Following ref.[19], the change of variables that would restore the symmetry is given by:

$$\begin{aligned} y_1 &= \sqrt{r^2 + q_1^2}\ \mu_1 \cos\phi_1 , \quad y_2 = \sqrt{r^2 + q_1^2}\ \mu_1 \sin\phi_1 , \quad y_3 = \sqrt{r^2 + q_2^2}\ \mu_2 \cos\phi_2 , \\ y_4 &= \sqrt{r^2 + q_2^2}\ \mu_2 \sin\phi_2 , \quad y_5 = \sqrt{r^2 + q_3^2}\ \mu_3 \cos\phi_3 , \quad y_6 = \sqrt{r^2 + q_3^2}\ \mu_3 \sin\phi_3 . \end{aligned} \tag{16}$$

In view of this, for the single charge case, one defines the following radial coordinate:

$$r = \frac{u^2 + \sqrt{u^2(u^2+q^2) - u_H^4}}{\sqrt{q^2 + 2u^2 + 2\sqrt{u^2(u^2+q^2) - u_H^4}}} . \tag{17}$$

This allows us to rewrite:

$$f^{-1} du^2 + R^2 d\theta^2 = R^2 \left(\frac{dr^2}{r^2 + q^2} + d\theta^2 \right) . \tag{18}$$

We can now define new coordinates:

$$\widetilde{L} = \sqrt{r^2 + q^2} \sin\theta , \quad \rho = r\cos\theta ,$$

so that we have:

$$R^2(\frac{dr^2}{r^2+q^2}+d\theta^2)=\frac{R^2}{\sqrt{4q^2\rho^2+(L^2+\rho^2-q^2)^2}}(d\widetilde{L}^2+d\rho^2)\ . \tag{19}$$

Then from the asymptotic behavior of r for large u:

$$\sqrt{r^2+q^2}=u+\frac{q^2}{2u}+\dots\ , \tag{20}$$

we can argue that $\widetilde{L}$ has the expansion:

$$\widetilde{L}=m+\frac{c+m\frac{q^2}{2}}{\rho^2}+\dots\ . \tag{21}$$

Using the standard argument from ref.[9] we can show that:

$$\langle\overline{\psi}\psi\rangle\sim -c-m\frac{q^2}{2}\ . \tag{22}$$

So, in these coordinates that restore the symmetry of the S^5, the naïve condensate value gets a constant subtraction. Henceforth, all future plots of $-c$ will subtract off this term. The adjusted solution and the phase transition region are shown in figure 6.

There are several important things to notice. First, in figure 6(a), unlike the AdS Schwarzschild case, we begin to see the condensate becoming negative for small bare quark mass. In addition, we see the appearance of *apparently* negative masses (see figure 7(a)) . This of course corresponds to negative $L=u\sin\theta$ value for $\rho\to\infty$. This effect is to be interpreted as the constant coordinate ϕ_1 flipping to $\pi-\phi_1$. This has been checked by extending θ to negative values and observing that we get the same physics, continued to the negative mass side. This is simply the familiar case of realizing that a negative radial coordinate should be flipped back to positive values after taking into account the range of the angular coordinates. Here, by considering the fixed ϕ_1 ansatz, we are required to extend the definition of θ to negative values. Therefore, these solutions would have physical values given by $m\to -m$ and $c\to -c$.

Therefore, we see the appearance of a finite condensate gap between the $(m=0,-c=0)$ solution and the $(m=0,-c\neq 0)$. Our equal area law, discussed in ref.[10], tells us that the lower branch, corresponding to negative values of the condensate, has the lowest energy. Therefore, the system chooses the $(m=0,-c\neq 0)$ solution. This means that the geometry breaks $U(1)$ chiral symmetry spontaneously. We plot the value of the condensate at zero bare quark mass in figure 7(b). We see that there is a minimum amount of charge that is needed before chiral symmetry is broken. We also notice that the condensate decreases toward zero asymptotically as $q\to\infty$.

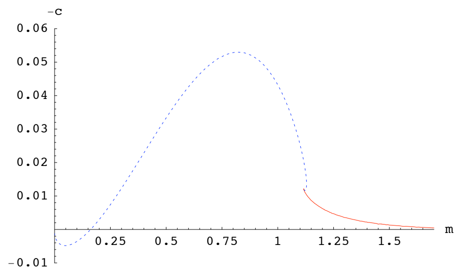

(a) Condensate (b) Energy

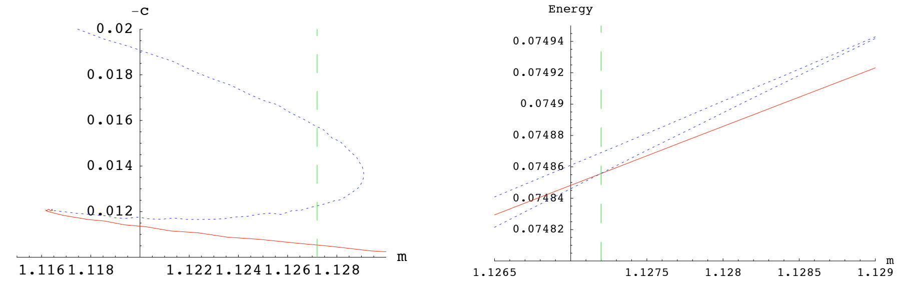

(c) Condensate in the transition region (d) Energy in the transition region

Figure 6: Solutions for one single charge in the transverse direction of the D7-brane for $q = 0.5$

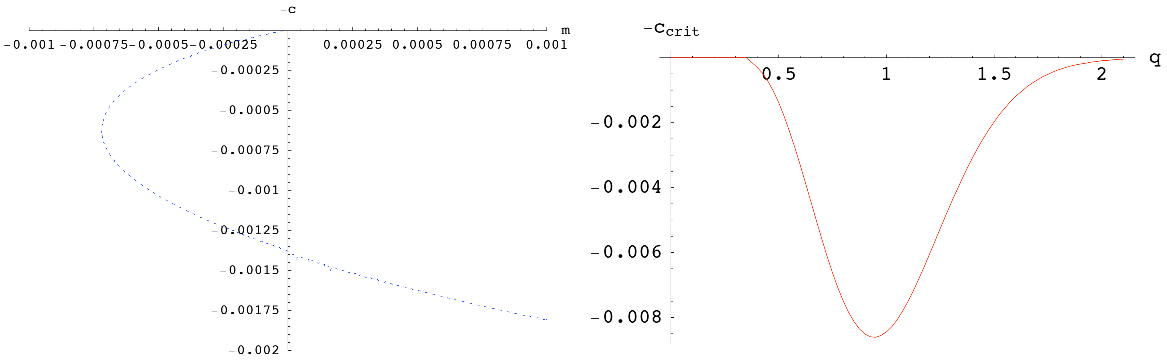

(a) Condensate near $m = 0$ for $q = 0.5$ (b) Condensate at $m = 0$ as a function of q

Figure 7: Behavior near $m = 0$ of the condensate for a single charge.

4 Three Equal Charges

When we set all three charges to be equal[5], ($i.e.,$ $q_1 = q_2 = q_3 = q$ in equation (3)), the metric is given by:

$$\begin{aligned} ds^2/\alpha' &= -\mathcal{H}^{-2} f dt^2 + \mathcal{H} f^{-1} du^2 + \mathcal{H}\frac{u^2}{R^2} d\vec{x}\cdot d\vec{x} \\ &\quad + \sum_{i=1}^{3}\left\{R^2 d\mu_i^2 + \mu_i^2\left(Rd\phi_i - Adt\right)^2\right\} \ , \end{aligned} \tag{23}$$

where

$$\mathcal{H} = 1 + \frac{q^2}{u^2} \ , \quad f = \frac{\mathcal{H}^3 u^2}{R^2} - \frac{u_H^4}{u^2 R^2} \ , \quad A = \frac{u_H^2 q}{R(u^2+q^2)} \ . \tag{24}$$

From a computational point of view, it is again more convenient to use

$$L(u) = u\sin\theta = m + \frac{c}{u^2} + O\left(\frac{1}{u^4}\right) \ . \tag{25}$$

However, just like in the single charge case of last section, the Karch–Katz–like solutions exhibit a positive slope of $q^2/2$ for the condensate, which is again an artifact of the coordinates. To show that, we introduce a new radial coordinate $r(u)$ satisfying:

$$\mathcal{H} f^{-1} du^2 + R^2 = \frac{R^2}{r^2}(dr^2 + r^2 d\theta^2) \ , \tag{26}$$

and the corresponding radial coordinates are:

$$\widetilde{L} = r\sin\theta \ , \quad \widetilde{\rho} = r\cos\theta \ . \tag{27}$$

Using that $r(u)$ from equation (26) has the asymptotic behavior:

$$r(u) = u + \frac{q^2}{2u} + O\left(\frac{1}{u^3}\right) \ , \tag{28}$$

one can show that:

$$\widetilde{L} = m + \left(c + m\frac{q^2}{2}\right)\frac{1}{\rho^2} + O\left(\frac{1}{\rho^4}\right) \ . \tag{29}$$

Note also that one can write:

$$\mathcal{H} f^{-1} du^2 + R^2 = \frac{R^2}{L^2+\rho^2}(d\rho^2 + dL^2) \ , \tag{30}$$

and following the standard argument presented in ref.[9] one can show that:

$$\langle\overline{\psi}\psi\rangle \sim -c - m\frac{q^2}{2} \ . \tag{31}$$

Therefore, to explore the functional dependence of the condensate on the bare quark mass, we again choose $\theta(z = 1/u^2)$ and ϕ_1 to be our transverse coordinates to the D7–brane. With this choice, the worldvolume of the D7–brane is given by:

$$\sqrt{-\det g} \;=\; (\det S_3)^{1/2}\,\frac{\cos^3\theta}{2z^3}\left|\frac{\mathcal{H}}{f}\left(f - A^2\mathcal{H}^2\sin^2\theta\right)\left(\mathcal{H} + 4R^2 f z^3\,(\theta')^2\right)\right|^{1/2} . \qquad (32)$$

We see that when $\theta = \pi/2$, the worldvolume goes to zero. This corresponds to the Karch–Katz–like solutions that we saw for the AdS Schwarzschild black hole and our single charge case. The other case where the worldvolume goes to zero is when:

$$R^2 z\left(f - A^2\mathcal{H}^2\sin^2\theta\right) = 1 + z\left(3q^2 - b^4 z + 3q^4 z + q^6 z^2\right) - b^4 q^2 z^3 \sin^2\theta(z) = 0 \; . \qquad (33)$$

This is a similar situation as for the single charge case, where the worldvolume goes to zero, but the D7–brane continues through and ends only at the event horizon determined by $G^{uu} = 0$. We can solve the equation of motion for θ numerically (using $R = u_H = 1$) using the same boundary conditions as in equation (12) for the Karch-Katz–like solutions and the curve in figure 8 for $\theta < \pi/2$, and we illustrate the two types of solutions in figure 9. We see exactly the same behavior as in the single charge; for large m, the slope of the $-c$ vs. m plot, (figure 9(b)) is given by $q^2/2$, as can be expected from the arguments presented above. Therefore, as in the single charge case we will henceforth subtract this $q^2/2$ contribution from all future $-c$ values displayed in our figures. Figure 10 shows solutions for a variety of charges. We can determine where the phase transition between condensate and Karch–Katz–like occurs from the equal-area law that we determined in ref.[10]. This allows us to avoid calculating the energy of the D7–brane. We again notice that, beyond a critical value of q, we begin to see solutions with

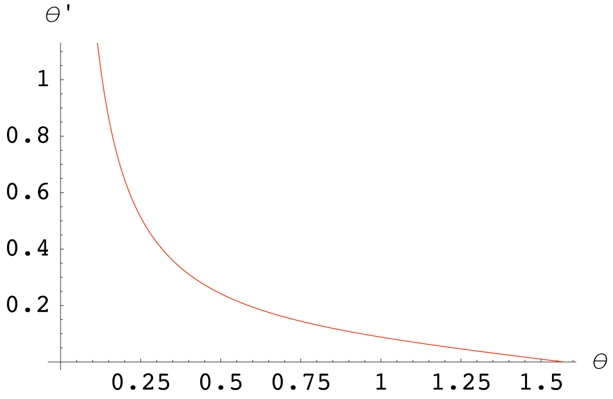

Figure 8: Boundary condition at the pseudo-horizon for $q = 0.5$.

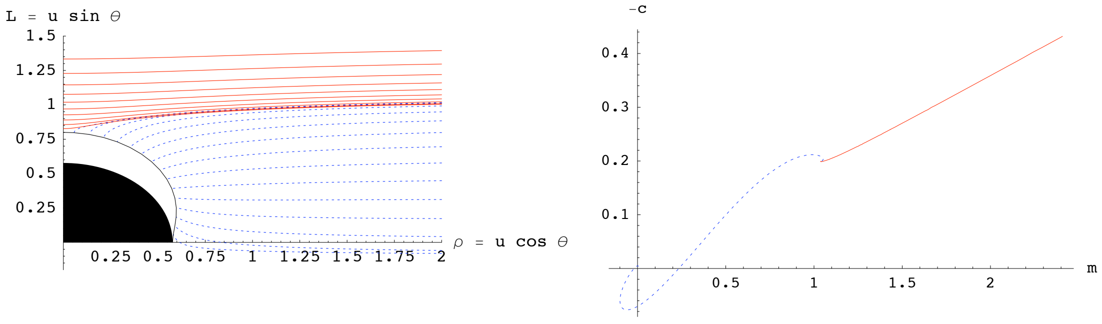

(a) (b)

Figure 9: Example of solutions for three equal $q = 0.6$ charges. The event horizon defined by $G^{uu} = 0$ is shown as the black disk. Again, the red solid lines correspond to Karch-Katz-like solutions and the blue dashed lines correspond to the condensate solutions.

negative condensate value (see figure 10(a)); we saw this feature in the single charge case as well.

Notice also that we again see the appearance of solutions with *apparently* negative bare quark mass; this of course corresponds to negative $L = u \sin\theta$ value for $\rho \to \infty$, an effect seen in figure 9(b) and can be explained as before. For those values, one simply swops $m \to -m$.

Therefore, we see the appearance of a discrete condensate gap between the $(m = 0, -c = 0)$ solution and the $(m = 0, -c \neq 0)$. Using our equal area law, it would tell us that the lower branch, corresponding to negative values of the condensate, has the lowest energy. This means that our gauge theory will choose to have a non-zero condensate at zero bare quark mass. This means the geometry breaks $U(1)$ chiral symmetry spontaneously. As q approaches its maximum value ($q \approx 0.62$) after which there is no event horizon, we begin seeing a multiplicity of condensate solutions for small bare quark mass, resulting from the rather beautiful spiral of solutions (see the first quadrant in figures 11(a) and 11(b). Using our equal area law again, we learn that the lowest branch of the spiral, corresponding to negative values of the condensate, has the lowest energy, and as we go “deeper” into the spiral every successive branch has higher energy; The other zero–mass condensates are simply metastable states. Therefore, again at zero bare quark mass, we have a non-zero negative condensate value and chiral symmetry breaking. We plot the condensate value for zero bare quark mass as a function of the charge q in figure 12. We see again that there is a minimum q below which chiral symmetry is unbroken.

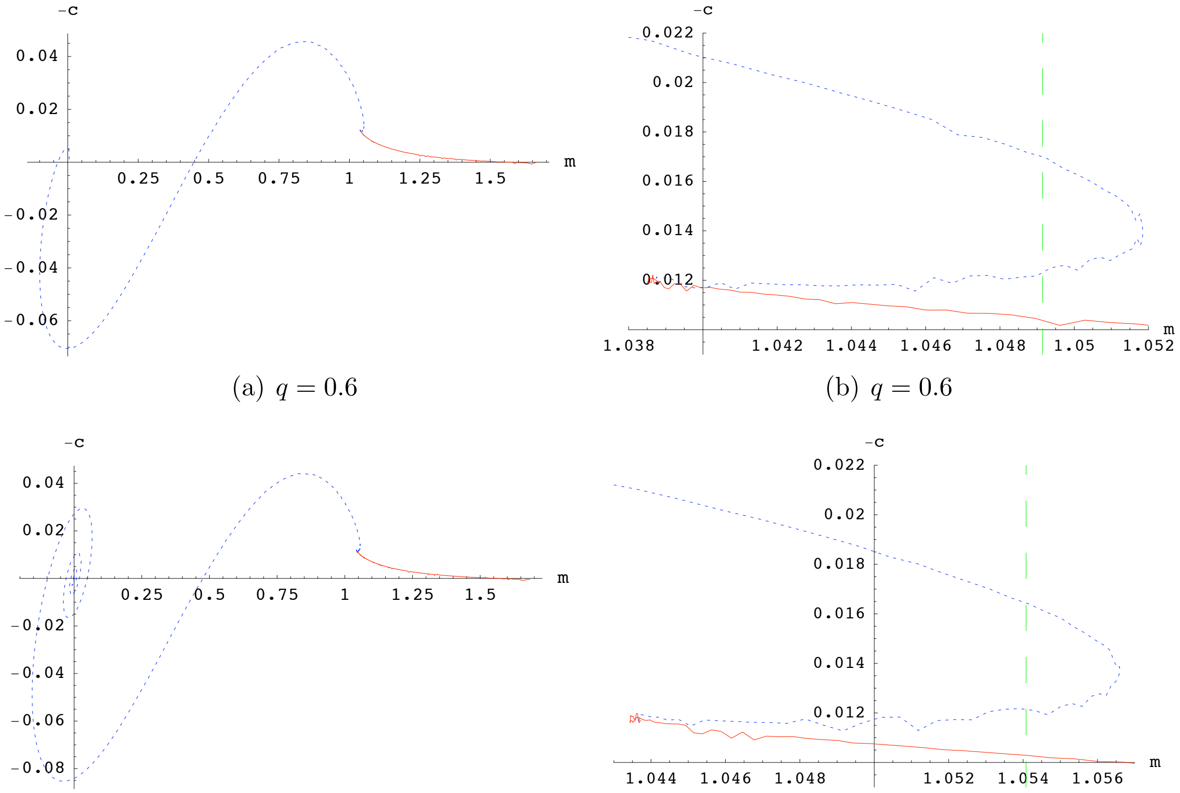

(a) $q = 0.6$

(b) $q = 0.6$

(c) $q = 0.62$

(d) $q = 0.62$

Figure 10: Solutions for three equal charges for various q. The dashed green line represents where the phase transition occurs.(In the dramatically magnified regions shown on the right, there is some jaggedness of the curves, as we are near the limit of our numerical accuracy. This should not be a cause for concern.)

5 Meson Spectrum

In order to confirm that we are indeed seeing chiral symmetry breaking, we calculate the quadratic fluctuations in the transverse coordinate ϕ_1 about the embedding solutions for $\theta(z)$ we found earlier. In the gauge theory, this will correspond to a pseudo-scalar meson, as described in ref.[9]. As a reminder, in ref. [20], the exact meson spectrum for the AdS$_5 \times S^5$ background was found to be given by:

$$M(n,\ell) \quad = \quad \frac{2m}{R^2}\sqrt{(n+\ell+1)(n+\ell+2)}\ , \tag{34}$$

where ℓ labels the order of the spherical harmonic expansion, and n is a positive integer that represents the order of the mode. In our meson spectrum calculations, we have only considered

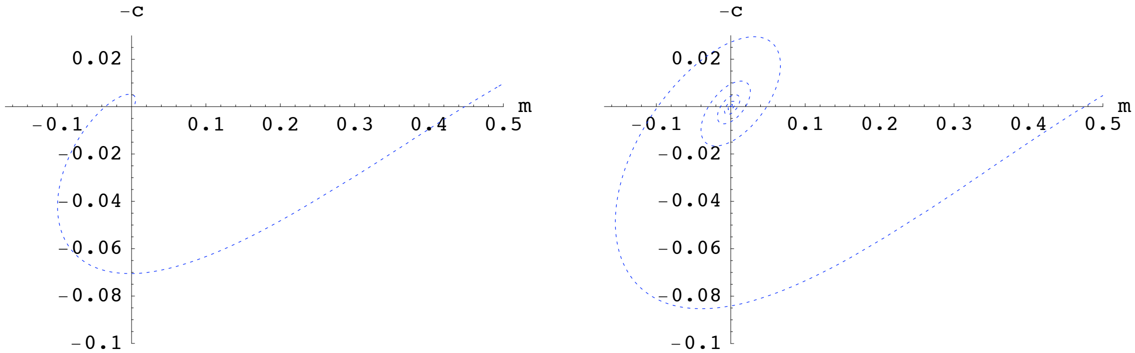

(a) $q = 0.6$ (b) $q = 0.62$

Figure 11: Zoom of the behavior near the origin of the condensate as a function of bare quark mass

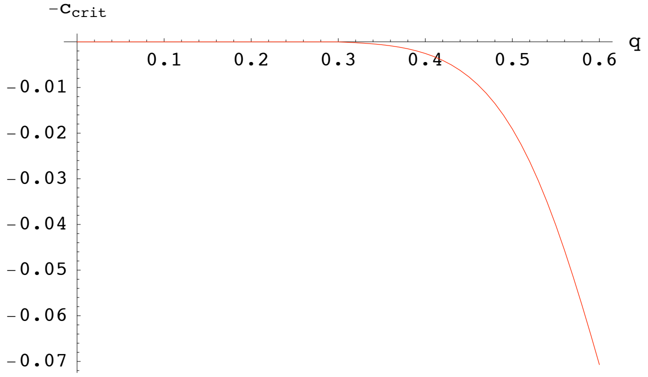

Figure 12: Value of the condensate for the three charge case at zero bare quark mass as a function of the magnitude of the charge

the $n = \ell = 0$ solutions for the fluctuations in θ and ϕ. We will choose an ansatz of the form:

$$\delta\phi_1 = \chi(z) \exp\left(-i\omega t\right) \ , \tag{35}$$

where Re$[\omega] = M$ corresponds to the meson's 4–dimensional mass and Im$[\omega]$ corresponds to the inverse of the meson's lifetime. We then recalculate the DBI action of the D7–brane probe and expand the action to second order in $\chi(z)$. The classical equations of motion for the fluctuation can then be derived using the Euler–Lagrange equation. The first thing we find is that near the event horizon, the equation of motion does not have the form of a Heun equation; this means that we do not have quasi–normal modes at the event horizon. This means that the condensate embeddings and the mesons associated with their fluctuations are stable. This is the opposite of what has been found for the AdS Schwarzschild black hole background [21, 22, 10]. Therefore, we only need to consider the real part of ω in our analysis. In order to solve for the mass of the meson, we again solve our equation of motion by shooting from where the worldvolume is zero towards infinity. Our boundary conditions for the condensate embeddings is determined by the equation of motion, as before to require that the function $\chi(z)$ is smooth across the vanishing worldvolume locus.

$$\begin{aligned} \chi(z)\big|_{\text{w.v.}\to 0} &= 10^{-3} \\ \chi'(z)\big|_{\text{w.v.}\to 0} &= \omega^2 \Theta(\theta) \ , \end{aligned} \tag{36}$$

where $\Theta(\theta)$ is shown in figure 13. Our boundary conditions for the Karch–Katz–like embeddings is simply given by:

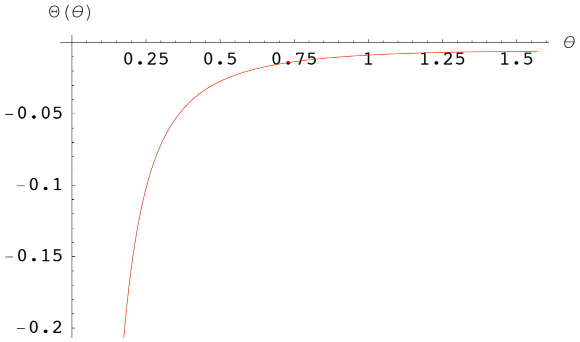

Figure 13: Boundary Condition function $\Theta(\theta)$ for the single charge case

$$\begin{aligned} \chi(z)\big|_{\text{w.v.}\to 0} &= 10^{-3} \\ \chi'(z)\big|_{\text{w.v.}\to 0} &= 0 \ . \end{aligned} \tag{37}$$

Solutions for the single charge case are shown in figure 14 for a case where we do not see chiral symmetry breaking and a case where we do see symmetry breaking. We see that for the case where we claimed to see a non-zero condensate at zero bare quark mass ($q = 0.7$), we definitely see a massless meson (see figure 14(b); for the case where we had no condensate at zero bare quark mass, we have no massless meson (see figure 14(a)). In addition, we plot the small m behavior of the meson in figure 15. If this is indeed the Goldstone boson associated with chiral symmetry breaking, it should obey the Gell-Mann–Oakes–Renner relation[16], which states that:

$$M_\pi = \sqrt{-m_q \langle \bar{\psi}\psi \rangle / f_\pi^2} \ , \tag{38}$$

where m_q is the bare quark mass, and f_π is the pion decay constant. We can fit our curve nicely with a square root function as:

$$M = 3.57342 \ m^{1/2} \ , \tag{39}$$

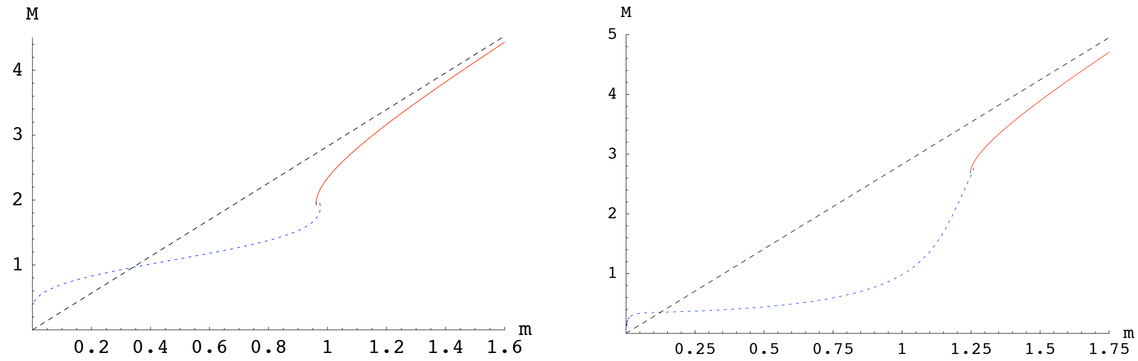

(a) $q = 0.2$ (b) $q = 0.7$

Figure 14: ϕ_1 Meson spectrum for the single charge. The dashed line is the solution for the $\mathrm{AdS}_5 \times S_5$ case.

which serves as a nice confirmation of our results.

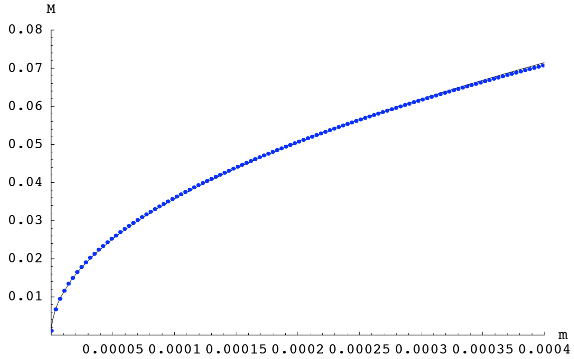

Figure 15: Small bare quark mass behavior of the single charge ϕ_1 meson. The black line is the $m^{1/2}$ best fit curve

We find we have very much the same results for the three charge case. The equations of motion do not form a Heun equation at the event horizon, so we have stable mesons. The boundary conditions are the same as in equations (36) and (37), with figure 16 showing the function $\Theta(\theta)$. Solutions for the three charge case are shown in figure 17 for a case where we do not see chiral symmetry breaking and a case where we do see symmetry breaking. We again find a massless meson in the case where we have a condensate at zero bare quark mass (see figure 17(b). In addition, we can fit the curve nicely for small bare quark mass (as shown in figure 18) as:

$$M = 3.45336\ m^{1/2}\ , \tag{40}$$

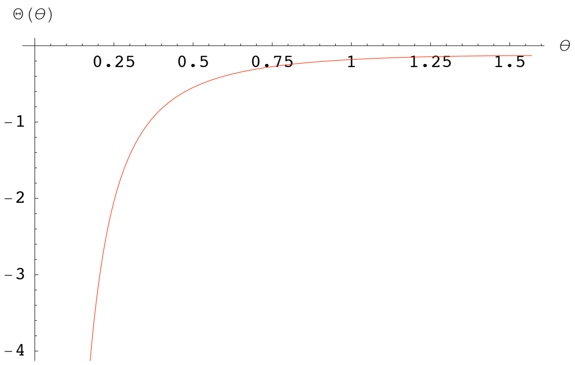

Figure 16: Boundary Condition function $\Theta(\theta)$ for the three charge case

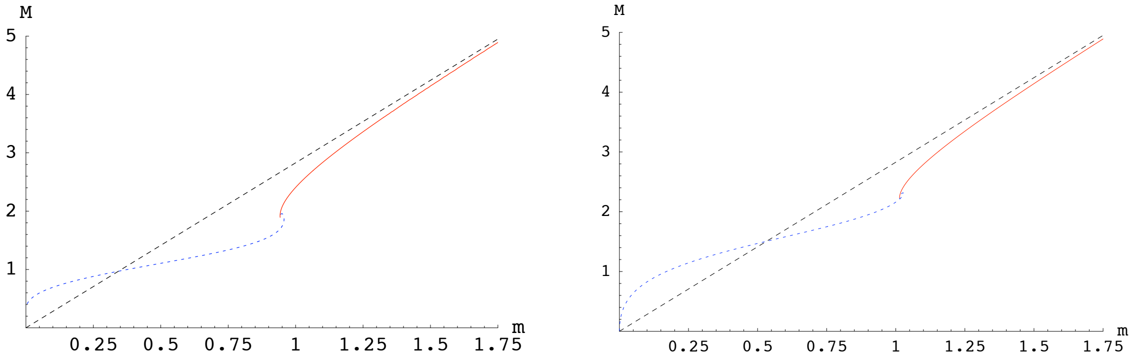

(a) $q = 0.2$

(b) $q = 0.5$

Figure 17: ϕ_1 Meson spectrum for the three charge. The dashed line is the solution for the $\mathrm{AdS}_5 \times S_5$ case.

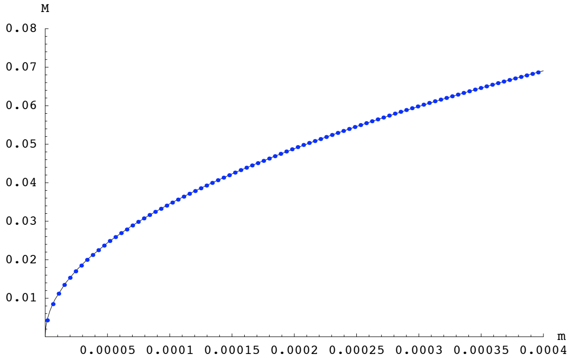

Figure 18: Small bare quark mass behavior of the three charge ϕ_1 meson. The black line is the $m^{1/2}$ best fit curve

once again confirming that we have chiral symmetry breaking beyond some critical value of q.

Acknowledgments

We are grateful to Nick Evans, Rob Myers, and Andreas Karch for comments. This research is supported by the US Department of Energy.

References

[1] J. M. Maldacena, "The large N limit of superconformal field theories and supergravity," *Adv. Theor. Math. Phys.* **2** (1998) 231–252, `hep-th/9711200`.

[2] E. Witten, "Anti-de Sitter space and holography," *Adv. Theor. Math. Phys.* **2** (1998) 253–291, `hep-th/9802150`.

[3] S. S. Gubser, I. R. Klebanov, and A. M. Polyakov, "Gauge theory correlators from non-critical string theory," *Phys. Lett.* **B428** (1998) 105–114, `hep-th/9802109`.

[4] E. Witten, "Anti-de Sitter space, thermal phase transition, and confinement in gauge theories," *Adv. Theor. Math. Phys.* **2** (1998) 505–532, `hep-th/9803131`.

[5] A. Chamblin, R. Emparan, C. V. Johnson, and R. C. Myers, "Charged AdS black holes and catastrophic holography," *Phys. Rev.* **D60** (1999) 064018, `hep-th/9902170`.

[6] A. Chamblin, R. Emparan, C. V. Johnson, and R. C. Myers, "Holography, thermodynamics and fluctuations of charged AdS black holes," *Phys. Rev.* **D60** (1999) 104026, `hep-th/9904197`.

[7] M. Cvetic and S. S. Gubser, "Thermodynamic stability and phases of general spinning branes," *JHEP* **07** (1999) 010, `hep-th/9903132`.

[8] A. Karch and E. Katz, "Adding flavor to AdS/CFT," *JHEP* **06** (2002) 043, `hep-th/0205236`.

[9] M. Kruczenski, D. Mateos, R. C. Myers, and D. J. Winters, "Towards a holographic dual of large-N(c) QCD," *JHEP* **05** (2004) 041, `hep-th/0311270`.

[10] T. Albash, V. Filev, C. V. Johnson, and A. Kundu, "A Topology-Changing Phase Transition and the Dynamics of Flavour," `hep-th/0605088`.

[11] J. Babington, J. Erdmenger, N. J. Evans, Z. Guralnik, and I. Kirsch, "Chiral symmetry breaking and pions in non-supersymmetric gauge / gravity duals," *Phys. Rev.* **D69** (2004) 066007, `hep-th/0306018`.

[12] A. Karch and A. O'Bannon, "Chiral Transition of N=4 Super Yang-Mills with Flavor on a 3-Sphere," `hep-th/0605120`.

[13] I. Kirsch, "Generalizations of the AdS/CFT correspondence," *Fortsch. Phys.* **52** (2004) 727–826, `hep-th/0406274`.

[14] K. Ghoroku, T. Sakaguchi, N. Uekusa, and M. Yahiro, "Flavor quark at high temperature from a holographic model," *Phys. Rev.* **D71** (2005) 106002, `hep-th/0502088`.

[15] D. Mateos, R. C. Myers, and R. M. Thomson, "Holographic Phase Transitions with Fundamental Matter," `hep-th/0605046`.

[16] M. Gell-Mann, R. J. Oakes, and B. Renner, "Behavior of current divergences under SU(3) x SU(3)," *Phys. Rev.* **175** (1968) 2195–2199.

[17] P. Kraus, F. Larsen, and S. P. Trivedi, "The Coulomb branch of gauge theory from rotating branes," *JHEP* **03** (1999) 003, `hep-th/9811120`.

[18] M. Cvetic *et al.*, "Embedding AdS black holes in ten and eleven dimensions," *Nucl. Phys.* **B558** (1999) 96–126, `hep-th/9903214`.

[19] J. G. Russo, "New compactifications of supergravities and large N QCD," *Nucl. Phys.* **B543** (1999) 183–197, `hep-th/9808117`.

[20] M. Kruczenski, D. Mateos, R. C. Myers, and D. J. Winters, "Meson spectroscopy in AdS/CFT with flavour," *JHEP* **07** (2003) 049, `hep-th/0304032`.

[21] C. Hoyos, K. Landsteiner, and S. Montero, "Holographic meson melting," `hep-th/0612169`.

[22] D. Mateos, R. C. Myers, and R. M. Thomson, "Thermodynamics of the brane," `hep-th/0701132`.